On Control of Static Synchronous Series Compensator for SSR Mitigation

Massimo Bongiorno, *Student Member, IEEE*, Jan Svensson, *Member, IEEE*, and Lennart Ängquist, *Member, IEEE*

***Abstract*—This paper deals with the analysis and simulation of the static series compensator (SSSC) for subsynchronous resonance (SSR) mitigation. The purpose of the paper is to derive and analyze a novel control strategy for SSSC dedicated for SSR mitigation. Objective of the proposed controller is to increase the network damping only at those frequencies that are critical for the turbine-generator shaft. By using frequency scanning analysis, the effectiveness of the proposed method for mitigation of SSR due to torsional interaction effect is presented and compared with the existing control strategy. Finally, simulation results show the performance of the proposed method in mitigating SSR due to torque amplification effect.**

***Index Terms*—Converters, current control, estimation, power systems, subsynchronous resonance (SSR).**

NOMENCLATURE

SSR	Subsynchronous Resonance.
IGE	Induction Generator Effect.
TI	Torsional Interaction.
TA	Torque Amplification.
FACTS	Flexible AC Systems.
STATCOM	Static Synchronous Compensator.
SSSC	Static Synchronous Series Compensator.
TCSC	Thyristor Controlled Series Capacitor.
FBM	First Benchmark Model.
PCC	Point of Common Coupling.
EA	Estimation Algorithm.
SSCC	Subsynchronous Current Controller.
PLL	Phase Locked Loop.
HP	High Pressure turbine stage.
IP	Intermediate Pressure turbine stage.
LP	Low Pressure turbine stage.
GEN	Generator.
EXC	Exciter.

Manuscript received July 20, 2007; revised October 10, 2007. This work was supported by ELFORSK under the Elektra program. Recommended for publication by Associate Editor J. Enslin.

M. Bongiorno is with the Department of Energy and Environment, Division of Electric Power Engineering, Chalmers University of Technology, Göteborg SE-412 96, Sweden (e-mail: massimo.bongiorno@chalmers.se).

J. Svensson and L. Ängquist are with the ABB Power Technologies, Västerås SE-721 57, Sweden (e-mail: jan.r.svensson@se.abb.com; lennart.angquist@se.abb.com).

Digital Object Identifier 10.1109/TPEL.2007.915178

I. INTRODUCTION

THE use of series capacitors in transmission lines can provide many benefits to improve the capability and the operation of the power systems. It was commonly believed until a few decades ago that series compensation up to 70% could be used in any transmission line without too many concerns. However, in 1971 it was discovered that using series capacitors can produce a significant adverse effect on thermal turbine-generator units connected to a series compensated power system. This phenomenon is referred to as subsynchronous resonance (SSR) [1]. SSR is a resonant condition, with frequency below the fundamental frequency, which is related to an energy exchange between the electrical and the mechanical system, coupled through the generator. SSR can be divided in two main groups [2]: steady state SSR (induction generator effect, IGE, and torsional interaction, TI) and transient torques [also known under the name of torque amplification (TA)]. IGE is considered as a theoretical condition that unlikely can occur in a series compensated power system, thus, it will not be considered in this paper. SSR due to TI and TA are dangerous conditions that can lead to shaft damage [3] and therefore must be avoided.

To avoid SSR in power systems, the use of FACTS Controllers such as the static synchronous compensator (STATCOM) [4], the static synchronous series compensator (SSSC) [5], [6] or the thyristor controlled series capacitor (TCSC) [7] has been proposed. In particular, the focus of this paper is on the control of the SSSC. The control strategy existing in the literature (referred to as "classical control"), is to inject a fundamental frequency voltage into the grid in order to shift the electrical resonance. However, the drawback of the classical control is that, depending on the grid impedance, large amount of power must be injected into the grid. The purpose of this paper is to investigate a novel control strategy for an SSSC dedicated for SSR mitigation. Effectiveness of the proposed control method to mitigate TI and TA effect will be presented and compared with the classical control strategy. The effect of the SSSC on the network damping and the impact of the controller parameters will be presented. Simulation results will prove that, with the proposed control system, the power rating of the SSSC can be drastically reduced, leading to a cost-effective solution for SSR mitigation.

II. SUBSYNCHRONOUS RESONANCE IN POWER SYSTEMS

In this section, conditions leading to SSR will be described. It is of importance to mention that while SSR due to TI effect can be analyzed analytically by using linear models, the analysis of SSR due TA is fairly complicated and can be approached only

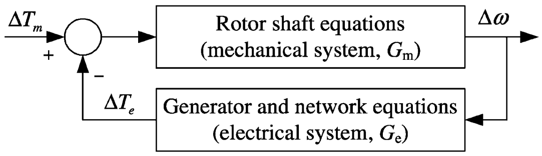

Fig. 1. Block scheme representing interaction between electrical and mechanical system.

by using a simulation program. The conditions that lead to SSR due TI effect will be analyzed. SSR due to TA is investigated in Section VII.

SSR due to TI effect can be investigated using the feedback loop depicted in Fig. 1, [8]. The mechanical system is typically constituted by several masses representing different turbine stages (low-pressure, intermediate-pressure, high-pressure) interconnected by elastic shafts. When a torsional mode is excited, the masses perform small amplitude twisting movements relative to each other. The phase angle of the generator mass becomes modulated, causing a variation in the stator flux ($\underline{\psi}_{\rm s}$). Depending on the series-compensated network, substantial modulation of the stator current ($\underline{i}$) will results. In particular, if the frequency of this oscillating current is electrically close to the resonance frequency of the series compensated network, undamped currents will result. The flux in the generator and the stator current will create an electrical torque $T_{\rm e}$ that will act on the generator mass. As a result, the feedback loop depicted in the figure is established.

Call $G_{\rm e}$ the transfer function from the rotor speed $\Delta\omega$ to the electrical torque $\Delta T_{\rm e}$

$$G_{\rm e}(s) = \frac{\Delta T_{\rm e}}{\Delta\omega}(s). \tag{1}$$

To investigate the response of the electrical system at different frequencies, the Laplace variable can be simply substituted with $\mathrm{j}\omega_k$, where ω_k is the frequency of interest (for example, one of the natural frequencies of the generator-shaft system). At each frequency, the transfer function $G_{\rm e}$ can be split up into its real and imaginary part, as

$$\begin{aligned} G_{\rm e}(\mathrm{j}\omega_k) &= \mathrm{Re}[G_{\rm e}(\mathrm{j}\omega_k)] + \mathrm{jIm}[G_{\rm e}(\mathrm{j}\omega_k)] = \\ &= \Delta T_{\rm De}(\mathrm{j}\omega_k) - \mathrm{j}\frac{\omega_{\rm B}}{\omega_k}\Delta T_{\rm Se}(\mathrm{j}\omega_k) \end{aligned} \tag{2}$$

with $\omega_{\rm B}$ the base frequency. The terms $\Delta T_{\rm De}$ and $\Delta T_{\rm Se}$ are named electrical damping and synchronizing torque, respectively. Similar definition holds for the mechanical damping and synchronizing torques, $\Delta T_{\rm Dm}$ and $\Delta T_{\rm Sm}$. In a series-compensated network, the electrical damping can be considered equal to zero for all frequencies except at the resonance of the electrical system [3], where $\Delta T_{\rm De}$ becomes negative. Assuming that the synchronizing torque is negligible, SSR due to TI occurs in the power system if $\Delta T_{\rm De}$ equals or is lower than the mechanical damping torque $\Delta T_{\rm Dm}$. A typical example that describes a situation with risk for SSR due to TI is depicted in Fig. 2, where the electrical and the mechanical damping torques for the IEEE First Benchmark Model (FBM) [9] are shown. In this example and in the following, the series capacitor is equal to 0.3 pu, corresponding to a series-compensation level of 60% of the 0.5 pu

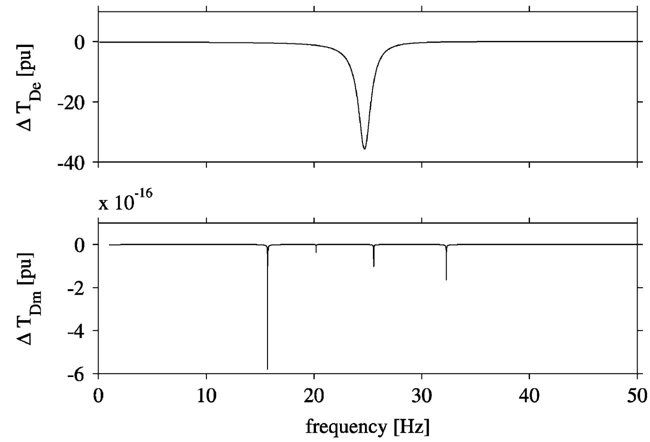

Fig. 2. Comparison between electrical damping torque ($\Delta T_{\rm De}$, upper plot) and mechanical damping torque ($\Delta T_{\rm Dm}$, bottom plot) for IEEE FBM. $X_{\rm c} = 0.3$ pu.

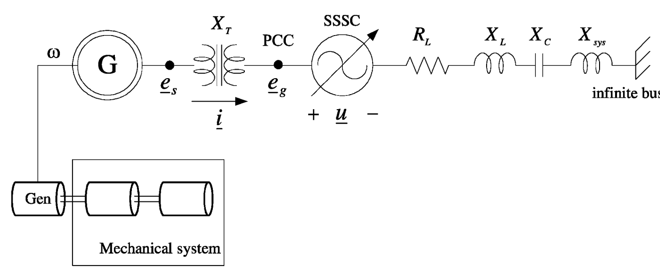

Fig. 3. Single-line diagram of power plant with generation unit and SSSC.

inductive reactance of the line. The electrical and the mechanical models are given in [3]. Observe from Fig. 2. that, due the selected level of series compensation, the electrical resonance occurs at 24.7 Hz. From the eigenvalue analysis of the mechanical system, the natural frequencies of the generator shaft are 15.71, 20.21, 25.55, 32.28 and 47.46 Hz. Therefore, the electrical resonance is close to one of the natural frequencies of the generator shaft. This might lead to a resonance between the electrical and the mechanical systems.

III. Classical Control of SSSC for SSR Mitigation

Fig. 3 shows the single-line diagram of a series-compensated transmission line with an SSSC installed downstream the step-up transformer located at the output of the power station. The voltage at the machine terminals is denoted by $\underline{e}_{\rm s}$, while the grid voltage at the Point of Common Coupling (PCC) and the grid current are denoted by $\underline{e}_{\rm g}$ and $\underline{i}$, respectively. The SSSC is modeled as a controlled ideal voltage source. The injected voltage is denoted by $\underline{u}$.

The principle of the SSR mitigation using the classical control is to replace the fundamental frequency voltage created by (at least a portion of) the inserted fixed capacitor banks by injecting a similar voltage that has been created by the SSSC. As the capacitive reactance from the capacitor bank is eliminated (or reduced), the electrical resonance of the system becomes shifted, thus avoiding the risk of SSR. The effectiveness of this control strategy has been described in several publications [10], [11] and has been proved both analytically and through real-time simulations. As an example, Fig. 4 shows the resulting damping

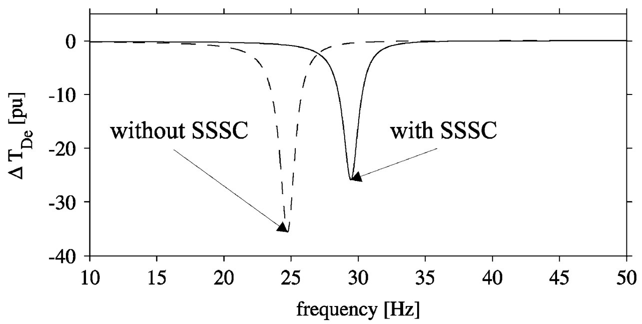

Fig. 4. Resulting electrical damping torque for IEEE FBM with SSSC. Classical control strategy has been adopted. Dashed curve: fixed series compensation only; solid curve: hybrid compensation (fixed capacitor and SSSC).

torque for the IEEE FBM when only fixed series compensation is used (dashed curve) and in case of hybrid compensation (fixed capacitor + SSSC, solid curve), wherein 45% of compensation is achieved by the fixed capacitor and the remaining 15% by the SSSC [12]. As shown, when hybrid compensation is used the characteristic frequency of the undamped pole has been moved from 24.7 to 29.4 Hz, which does not coincide with any of the torsional modes. Thus, this control strategy moves the undamping parts to frequencies that are not of danger for the generator-shaft system. Although effective, the drawback is that the SSSC must continuously inject reactive power into the system, regardless the presence or not of SSR. Moreover, depending on the system parameters, large amount of reactive power must be injected in the system in order to change the electrical impedance seen from the generator terminals.

In the following, a different approach for controlling the SSSC for SSR mitigation will be presented.

IV. Proposed Control of SSSC for SSR Mitigation

As shown in Fig. 2 (bottom plot), the turbine-generator shaft is characterized by sharp and poorly damped resonant points. The basic idea behind the proposed control algorithm is to increase the network damping only at those frequencies that are critical for the turbine-generator shaft. This is achieved by controlling the line current component at subsynchronous frequencies to zero. Since the natural frequencies of the generator-turbine shaft system can be considered to be constant with time [2], this method will allow decoupling the mechanical and electrical systems, regardless the configuration of the power system.

A. Subsynchronous Components Estimation Algorithm (EA)

When the generator rotor oscillates around its rated speed, the voltage at the terminals can be expressed in the synchronous (with undisturbed rotor position) dq-coordinate systems as [3]

$$\underline{e}_{\mathrm{s}}^{(dq)}(t) = \underline{e}_{\mathrm{s,f}}^{(dq)}(t) + \underline{e}_{\mathrm{s,sub}}^{(dq)}(t) + \underline{e}_{\mathrm{s,sup}}^{(dq)}(t) \tag{3}$$

where the subscripts "f", "sub" and "sup" denote the fundamental, the subsynchronous and the supersynchronous component of the measured grid voltage, respectively. As explained in [3], the network presents a small positive damping for frequencies above the fundamental. Therefore, the supersynchronous component is not of interest in this paper. The subsynchronous voltage rotates clockwise in the synchronous reference frame. Assume that the generator rotor oscillates with angular frequency ω_{m}. The dq_{m}-plane denotes a new set of coordinate systems that rotates synchronously with the subsynchronous voltage vector, (3) can be rewritten as

$$\underline{e}_{\mathrm{s}}^{(dq)}(t) = \underline{e}_{\mathrm{s,f}}^{(dq)}(t) + \underline{e}_{\mathrm{s,sub}}^{(dq_{\mathrm{m}})}(t)\mathrm{e}^{-\mathrm{j}(\omega_{\mathrm{m}}t)}. \tag{4}$$

In order to extract the subsynchronous component from the measured signal, (4) can be rearranged so that $\underline{e}_{\mathrm{s,f}}^{(dq)}$ and $\underline{e}_{\mathrm{s,sub}}^{(dq_{\mathrm{m}})}$ become isolated and then applying low-pass filtering on the resulting expression [13], [14]. Denote the estimated quantities with the superscript $\widehat{\ }$, the estimation algorithm (EA) can be expressed as follows:

$$\widehat{\underline{e}}_{\mathrm{s,f}}^{(dq)}(t) = H_{\mathrm{f}}(p)\left[\underline{e}_{\mathrm{s}}^{(dq)}(t) - \widehat{\underline{e}}_{\mathrm{s,sub}}^{(dq_{\mathrm{m}})}(t)\mathrm{e}^{-\mathrm{j}(\omega_{\mathrm{m}}t)}\right] \tag{5}$$

$$\widehat{\underline{e}}_{\mathrm{s,sub}}^{(dq_{\mathrm{m}})}(t) = H_{\mathrm{sub}}(p)\left[\underline{e}_{\mathrm{s}}^{(dq)}(t)\mathrm{e}^{\mathrm{j}(\omega_{\mathrm{m}}t)} - \widehat{\underline{e}}_{\mathrm{s,f}}^{(dq)}(t)\mathrm{e}^{\mathrm{j}(\omega_{\mathrm{m}}t)}\right] \tag{6}$$

where, indicating with p the operator $(\mathrm{d}/\mathrm{d}t)$, $H_{\mathrm{f}}(p)$ and $H_{\mathrm{sub}}(p)$ represent the transfer function of a low-pass filter for the fundamental and for the subsynchronous component, respectively. Equation (6) can be written in the synchronous dq-frame, yielding

$$\widehat{\underline{e}}_{\mathrm{s,sub}}^{(dq)}(t) = H_{\mathrm{sub}}(p + \mathrm{j}\omega_{\mathrm{m}})\left[\underline{e}_{\mathrm{s}}^{(dq)}(t) - \widehat{\underline{e}}_{\mathrm{s,f}}^{(dq)}(t)\right]. \tag{7}$$

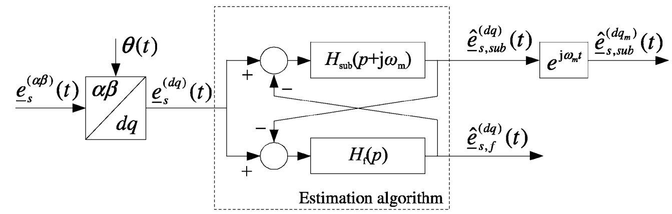

Fig. 5. Block diagram of subsynchronous components estimation algorithm.

Equations (5) and (7) can, thus, be combined together in order to extract the fundamental and the subsynchronous components of the measured voltage, as shown in Fig. 5, where the block diagram of the described EA is depicted. Fig. 6 displays the frequency response (gain and phase-shift) from $\underline{e}_{\mathrm{s}}^{(dq)}$ to $\underline{e}_{\mathrm{s,sub}}^{(dq)}$ of the EA when first-order low-pass filters are used. The oscillation frequency is assumed to be equal to 20.0 Hz ($\omega_{\mathrm{m}} = 125.66$ rad/s). The cutoff frequency of the filters (f_{cut}) has been set to 1 Hz both for $H_{\mathrm{f}}(p)$ and $H_{\mathrm{sub}}(p)$. Observe that the EA has the same behavior as a resonant filter with center frequency at ω_{m}. The algorithm presents a 1 pu gain with zero phase-shift at the frequency ω_{m}. Then, the gain rapidly decreases for all other frequencies. The selectivity of the detection algorithm, i.e., the sharpness of the peak, depends on the selected cutoff frequency of the filters. In the following, the superscript $\widehat{\ }$ denoting estimated quantities will be omitted.

B. Subsynchronous Current Controller (SSCC)

In this investigation, the generator can be modeled as an ideal voltage source behind the subtransient inductance of the generator [14]. To be able to control the subsynchronous current to

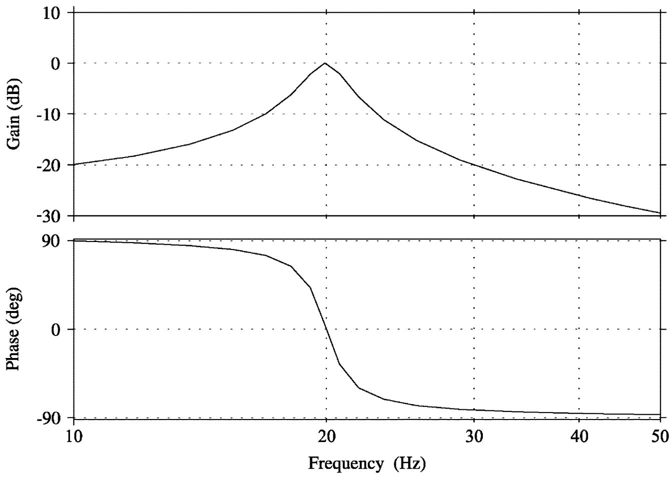

Fig. 6. Frequency response of estimation algorithm from $\underline{e}_{\mathrm{s}}^{(dq)}$ to $\underline{e}_{\mathrm{s,sub}}^{(dq)}$. First-order low-pass filters have been used. Top: gain; bottom: phase-shift.

zero, the objective of the control system is to rebuild the subsynchronous component of the internal bus voltage. Assume that the voltage downstream the SSSC is equal to zero, i.e., the voltage drop over the impedance downstream the compensator is treated as a disturbance. With the signal references given in Fig. 3, the law governing the subsynchronous current controller (SSCC) can be written in the Laplace domain as

$$\begin{aligned}\underline{u}_{\mathrm{sub}}^{(dq_{\mathrm{m}})}(s) &= \underline{e}_{\mathrm{g,sub}}^{(dq_{\mathrm{m}})}(s) + [R + \mathrm{j}(\omega - \omega_{\mathrm{m}})(L_{\mathrm{T}} + L'')]\underline{i}_{\mathrm{sub}}^{(dq_{\mathrm{m}})}(s) \\ &\quad + \left(K_{\mathrm{p}} + \frac{K_{\mathrm{i}}}{s}\right)\left[\underline{i}_{\mathrm{sub}}^{(dq_{\mathrm{m}})}(s) - \underline{i}_{\mathrm{sub}}^{(dq_{\mathrm{m}})*}(s)\right] \qquad (8)\end{aligned}$$

where R, L_{T} and L'' are the resistance of the system upstream the SSSC (i.e., the sum of the stator resistance of the generator and the series resistance of the transformer), the leakage inductance of the transformer and the subtransient inductance of the generator, respectively. The current reference is $\underline{i}_{\mathrm{sub}}^{(dq_{\mathrm{m}})*}$, while K_{p} and K_{i} are the proportional and the integral gains of the PI-regulator, respectively. To select the regulator gains, the closed-loop transfer function from $\underline{i}_{\mathrm{sub}}^{(dq_{\mathrm{m}})*}$ to the actual current $\underline{i}_{\mathrm{sub}}^{(dq_{\mathrm{m}})}$ can be shaped as a first-order low-pass filter, where the cutoff frequency of the filter corresponds to the bandwidth of the controller [15]. Thus, calling α_{cc} the bandwidth of the SSCC, the gains become equal to $K_{\mathrm{p}} = \alpha_{\mathrm{cc}} L$ (with $L = L_{\mathrm{T}} + L''$) and $K_{\mathrm{i}} = \alpha_{\mathrm{cc}} R$. Fig. 7 shows the block diagram of the proposed control system. Measured three-phase quantities are transformed to the fixed $\alpha\beta$-plane (not shown for clarity of the figure) and then to the synchronous reference frame by using the grid voltage angle θ, obtained from the PLL. The estimated subsynchronous components of voltage and current are transformed from the dq-to the dq_{m}-reference frame using the transformation angle θ_{m}, obtained from the integration of ω_{m}. The obtained quantities are then sent to the SSCC described in (8).

Observe that the block diagram in Fig. 7 is derived under the assumption that the rotor shaft has only one natural frequency, i.e., is constituted by only two masses (generator and one turbine stage). If more than two shaft-sections are present, such as for

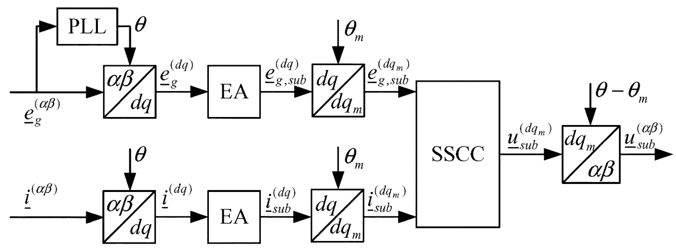

Fig. 7. Block-scheme of proposed control system.

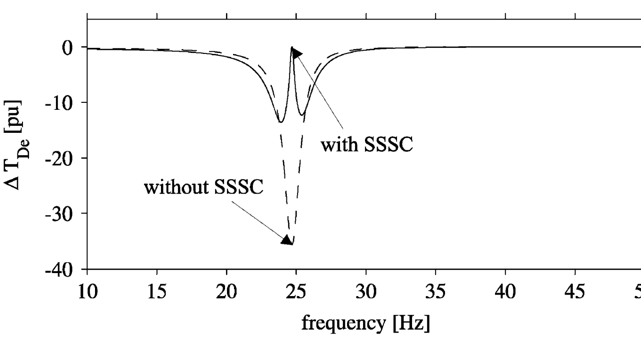

Fig. 8. Resulting electrical damping torque for investigated system with proposed control strategy. Dashed curve: SSSC in idle mode; solid curve: SSSC online.

the IEEE FBM, the complete control system will be constituted by several controllers as the one displayed in Fig. 7 (one for each natural frequency of the generator-turbine shaft system) connected in parallel.

V. Frequency Scanning Analysis

It is of interest to observe how the electrical damping torque ΔT_{De} is modified when the SSSC with the proposed control strategy is connected to the grid. Assume that the generator shaft has a natural frequency at 24.7 Hz, coinciding with an electrical resonance of the grid (at the complementary frequency $60-24.7 = 35.3$ Hz). Fig. 8 shows a comparison between the resulting damping torque for the investigated system when the compensator is in idle mode (dashed curve) and when the compensator is online (solid curve). The bandwidth of the SSCC, α_{cc}, is set to 10.45 rad/s [16], while $f_{\mathrm{cut}} = 1$ Hz. As shown, when the SSSC is online, the pole corresponding to the system undamping has been split into two new poles located in the sidebands of the original pole (23.92 and 25.4 Hz). The damping torque at the critical frequency for the generator shaft ω_{m} is equal to zero. In this way, the risk of SSR due to TI can be avoided. When comparing with the classical control strategy (see Fig. 4), the proposed control system SSSC will act only at the critical frequency ω_{m}. Thus, providing SSR mitigation by injecting a low amount of voltage into the grid, resulting in a reduced power rating of the compensator.

A. *Impact of Controller Parameters Variation on Damping Torque*

In this section, the impact of controller parameters variation over the resulting damping torque will be investigated.

1) Impact of SSCC: First, the impact of the SSCC bandwidth on the resulting damping torque will be considered. In

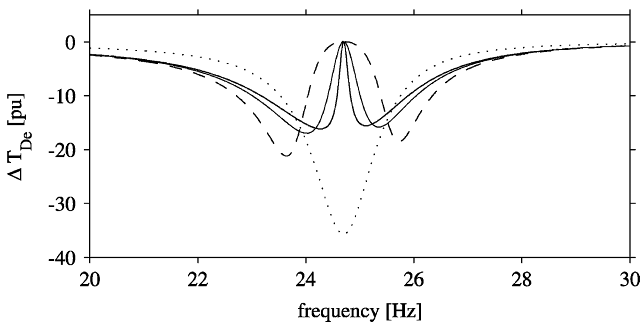

Fig. 9. Resulting damping torque for investigated system with proposed control strategy. Impact of α_{cc} variation. Dotted curve: SSSC in idle mode. Solid black curve: SSSC online, $\alpha_{cc} = 6$ rad/s. Solid gray curve: SSSC online, $\alpha_{cc} = 10$ rad/s. Dashed curve: SSSC online, $\alpha_{cc} = 14$ rad/s.

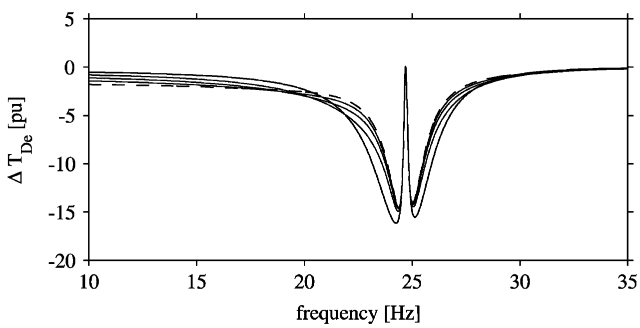

Fig. 10. Resulting damping torque for investigated system with proposed control strategy. SSSC online. Impact of EA when varying f_{cut} from 1 Hz (solid curve) to 5 Hz (dashed curve) in steps of 1 Hz.

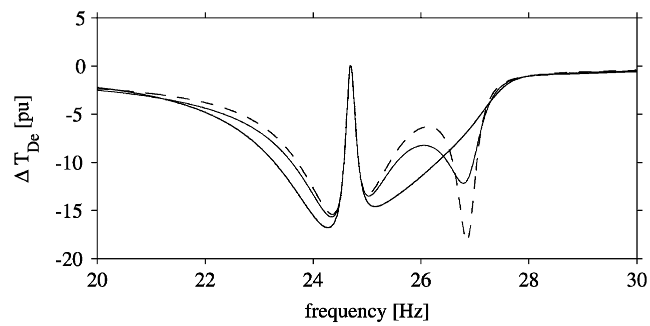

Fig. 11. Resulting damping torque for investigated system with proposed control strategy. SSSC online. Two subsynchronous frequency components are detected. Solid curve: $f_{cut} = 1$ Hz; gray curve: $f_{cut} = 2$ Hz; dashed curve: $f_{cut} = 3$ Hz.

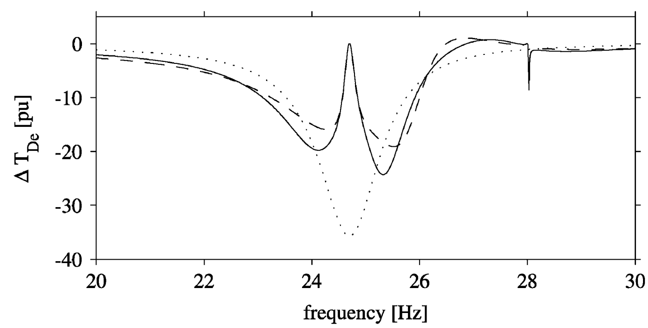

Fig. 12. Resulting damping torque for investigated system with proposed control strategy. SSSC online. Two subsynchronous frequency components are detected and controlled. Dotted curve: SSSC in idle mode; solid curve: SSSC online, $f_{cut} = 0.5$ Hz; dashed curve: SSSC online, $f_{cut} = 1$ Hz.

case of multi-mass generator shaft system, the bandwidth α_{cc} must be selected so that the controller in (8) acts at the selected frequency only. Therefore, since the natural frequencies of the generator shaft are typically close to each other, low bandwidth for the SSCC must be selected. In particular, for the IEEE FBM the stability margin is reached for $\alpha_{cc} = 14.5$ rad/s [16]. Fig. 9 shows the effect of the variation of the SSCC bandwidth over the resulting damping torque. The bandwidth α_{cc} has been varied from 6 to 14 rad/s. The cutoff frequency of the filters in the EA is set equal to 1 Hz. From the figure it is possible to observe that an increased bandwidth in the SSCC will result in a wider range of frequencies where the controller will modify the damping torque. Note that the two undamped poles located at the sidebands of ω_m move away from the controlled frequency when α_{cc} increases. Moreover, the undamping of these poles increases with α_{cc}. Therefore, since SSR is typically a slow phenomenon, low bandwidth for the SSCC is suggested.

2) Impact of EA: Also the cutoff frequency of the filters in the EA will impact on the resulting damping torque. With $\alpha_{cc} = 10$ rad/s, Fig. 10 shows the resulting damping torque when varying f_{cut} from 1 to 5 Hz (in steps of 1 Hz). Observe that the variation of f_{cut} affects the resulting damping torque only at low frequencies, where ΔT_{De} decreases with f_{cut}.

The variation of f_{cut} has a greater impact on ΔT_{De} when more than one subsynchronous frequency is detected. In practical implementation, the generator-turbine shaft system is constituted by several turbine stages coupled on the same shaft system [9]. Assume that there are two subsynchronous frequency components, one at 24.7 Hz and one at 28 Hz. For simplicity, only the subsynchronous current having characteristic frequency equal to 24.7 Hz is controlled to zero. From Fig. 11 it can be observed that an increase in f_{cut} will result in a new negative electrical damping at 26.85 Hz. This undesired effect is due to the inaccuracy of the EA in the frequency interval between the considered subsynchronous frequencies. Accordingly, in order to obtain a good selectivity of the EA, the selection of the cutoff frequency of the filters must be done with carefulness. When a multi-mass shaft system is considered, it is suggested to select f_{cut} no greater than one-fifth of the minimum frequency interval between two subsequent natural frequencies of the turbine-generator shaft system [13].

If also the subsynchronous current component at 28 Hz is controlled to zero, the resulting damping torque is modified as in Fig. 12. As shown, ΔT_e is set to zero also at 28 Hz. Due to the operation of the SSCC, a new undamped pole at 28.1 Hz can be observed. However, this frequency does not represent a risk for the turbine-generator shaft.

VI. Eigenvalue Analysis

It has been shown in the previous section that the effect of the proposed control system is to increase the network damping at the selected frequency. The effectiveness of the proposed control strategy when mitigating SSR due to TI effect can also be investigated from an eigenvalue analysis of the closed-loop

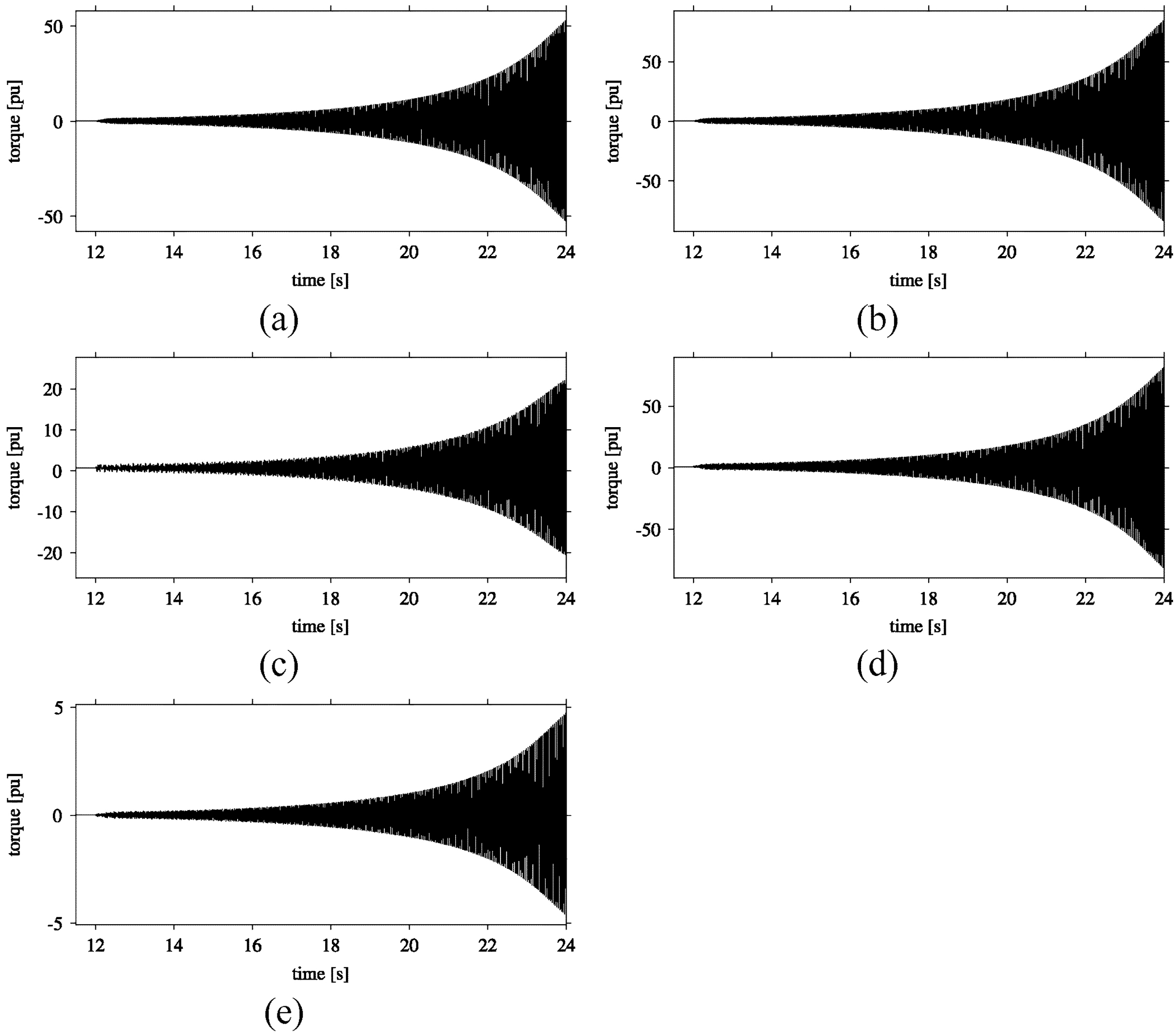

Fig. 13. Simulated generator shaft torques for IEEE FBM. SSSC in idle mode. Plot a: HP-IP torque; Plot b: $\mathrm{IP} - \mathrm{LP}_{\mathrm{A}}$ torque; Plot c: $\mathrm{LP}_{\mathrm{A}} - \mathrm{LP}_{\mathrm{B}}$ torque; Plot d: LP_{B}-GEN torque; Plot e: GEN-EXC torque.

TABLE I
CALCULATED EIGENVALUES FOR IEEE FBM

without SSSC		with SSSC	
Re [s^{-1}]	Im [rad/s]	Re [s^{-1}]	Im [rad/s]
−4.35	±598.68	−4.35	±598.68
−2.2 e^{-17}	±298.18	−1.47 e^{-6}	±298.18
0.007	±202.82	−0.007	±202.82
0.52	±160.03	−0.0006	±160.57
−4.95	±155.58	−3.97	±156.57
0.01	±127.04	−7.17	±127.5
0.043	±99.54	−0.06	±98.97

system in Fig. 1. Table I shows the eigenvalues (real and imaginary part) of the IEEE FBM without and with the SSSC. The SSCC bandwidth is equal to 10 rad/s, while $f_{\mathrm{cut}} = 1$ Hz. As shown, due to the selected series-compensation level (60%), the closed-loop system without SSSC presents four unstable poles. The inclusion of the SSSC leads to a stable system, thus reducing the risk of SSR.

VII. SIMULATION RESULTS

In the previous sections, the effectiveness of the investigated control algorithm to mitigate SSR due to TI has been shown. To investigate the effectiveness of the proposed control strategy also for mitigation of SSR due to TA, the IEEE FBM with SSSC has been simulated using the simulation program PSCAD/EMTDC. To be implemented in a digital controller, the EA and the SSCC have been discretized with sampling time $T_{\mathrm{s}} = 0.83$ ms, corresponding to a sampling frequency $f_{\mathrm{s}} = 1.2$ kHz. With the SSSC in idle mode, Fig. 13 shows the resulting torques between the different sections of the generator-shaft system when a three-phase fault is applied in the power system. As shown, very high torques will be experienced, leading to shaft failure. With the SSSC active, the system will react to control the subsynchronous components of the line current to zero. Fig. 14 shows the estimated subsynchronous line currents in the corresponding dq_{m}-coordinate systems. As expected from the eigenvalue analysis (see Table I, left column), due to the selected series-compensation level, the dominant subsynchronous frequency component is the third one, equal to 25.55 Hz ($\omega_{\mathrm{m}} = 160.53$ rad/s). As shown in Fig. 14(c), this subsynchronous current is equal to zero before the fault. After the fault is cleared, the subsynchronous current raises up to 0.5 pu. Then, the SSSC slowly controls this current

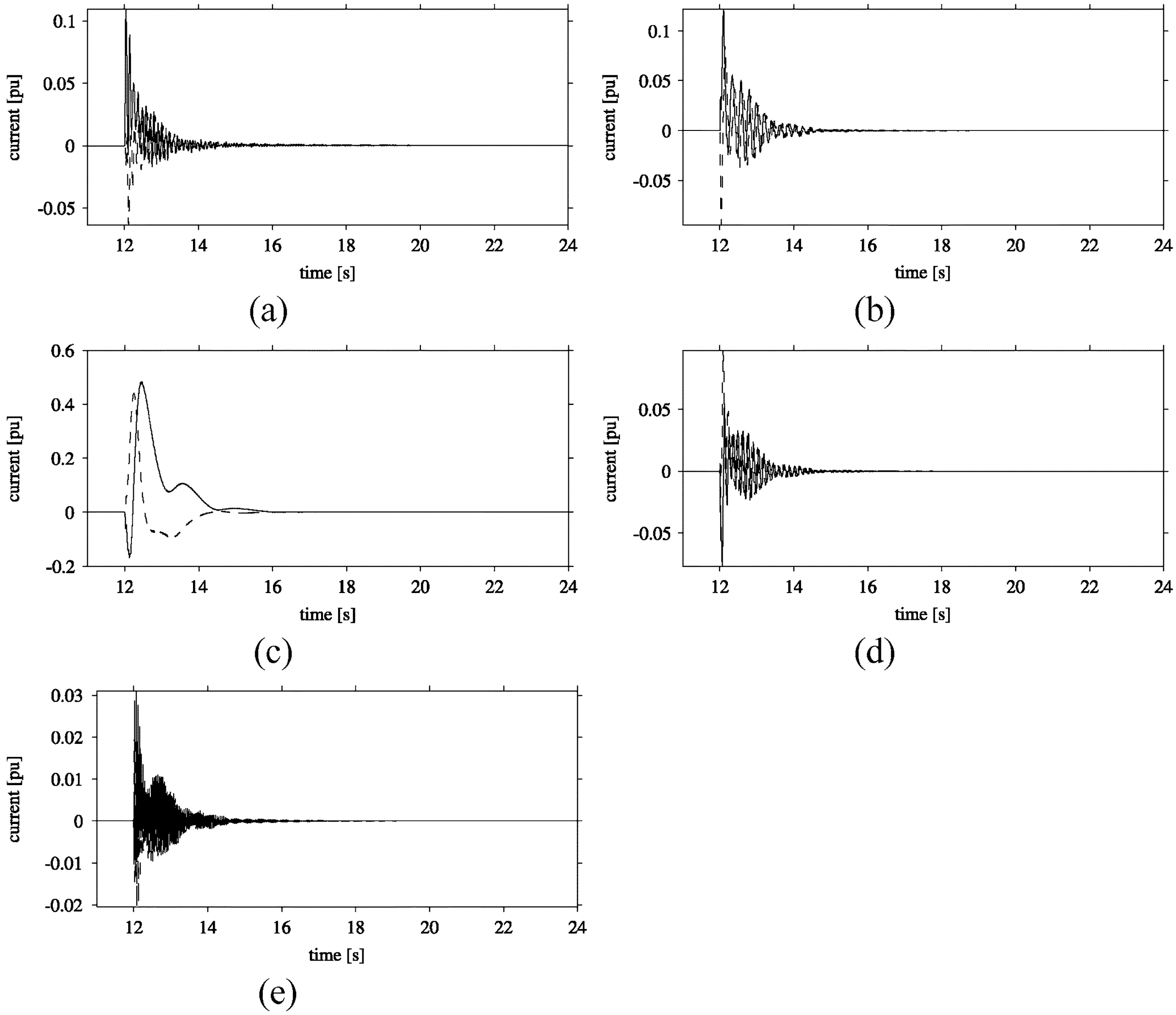

Fig. 14. Estimated subsynchronous currents in corresponding subsynchronous reference frames. Dashed curve: d_{m}-component; solid curve: q_{m}-component. Plot a: $\omega_{\mathrm{m}} = 98.71$ rad/s. Plot b: $\omega_{\mathrm{m}} = 126.98$ rad/s. Plot c: $\omega_{\mathrm{m}} = 160.53$ rad/s. Plot d: $\omega_{\mathrm{m}} = 202.82$ rad/s. Plot e: $\omega_{\mathrm{m}} = 298.2$ rad/s.

component to zero. As a result, the turbines of the generator shaft will still experience oscillations due to the fault, but they will be damped and go back to the pre-fault value, as displayed in Fig. 15. From the figure it can be observed that the maximum peak torque will be experienced between the second low-pressure turbine and the generator, with a maximum peak of 3 pu. However, this peak torque will persist for a few cycles only, therefore it does not represent a risk for the generator shaft [17].

It is of interest to investigate the effect of the variation of the bandwidth α_{cc} on the overall performance of the system. Fig. 16 shows the trend of the voltage injected by the SSSC (top plot, expressed in percent of the rated phase-to-ground voltage of the system), of the peak $\mathrm{LP_B} - \mathrm{GEN}$ torque (middle plot) and of the time required to damp the oscillations (here named "damping time," bottom plot) as a function of α_{cc}. The bandwidth has been varied from 6.28 to 14.5 rad/s. A first important conclusion is that, with the proposed approach, SSR mitigation is achieved with very low voltage injection. As shown in the figure, the maximum voltage injected by the SSSC into the grid is only 1% of the rated voltage of the system. As expected, the injected voltage (thus, the ratings of the SSSC) increases with α_{cc}. Vice versa, the peak torque and the damping time decrease when α_{cc} increases. From the figure it can be observed that the choice of $\alpha_{\mathrm{cc}} = 10$ rad/s represents a good compromise between system performance and ratings of the SSSC.

VIII. Conclusion

In this paper, the use of the SSSC for SSR mitigation has been treated. As first, the classical control strategy for SSR mitigation has been described. Then, a novel control strategy, based on the use of a subsynchronous current controller (SSCC) has been explained. An algorithm for online estimation of subsynchronous components in the measured signals has been proposed. Frequency scanning analysis of the investigated system has been carried out. The impact of controller parameters variation over the resulting damping torque has been shown. It has been shown that with the proposed control strategy, successful mitigation of SSR due to TI and TA effect is obtained. SSR mitigation is

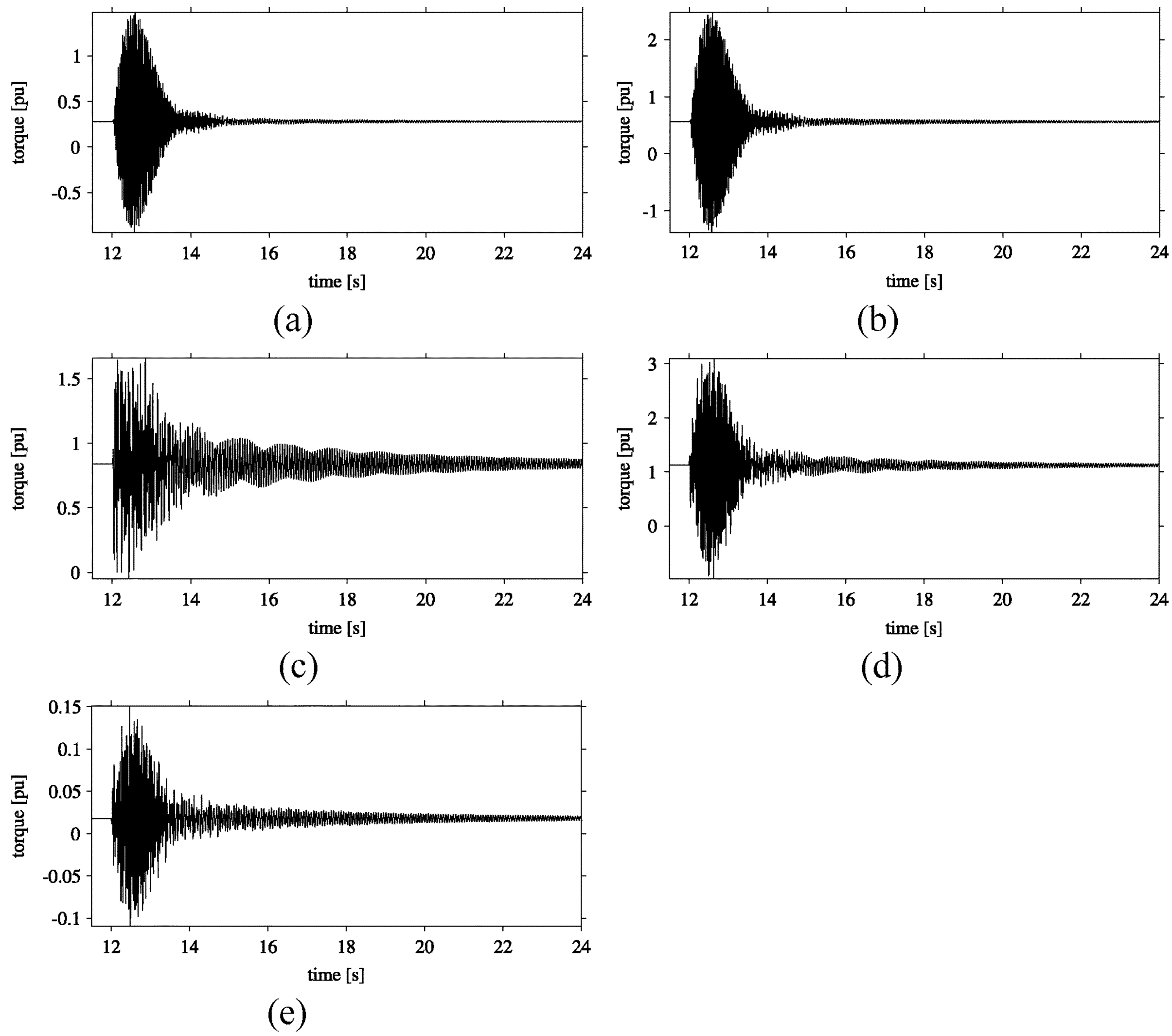

Fig. 15. Simulated generator shaft torques for IEEE FBM. SSSC online. Plot a: HP-IP torque; Plot b: IP-LP_{A} torque; Plot c: $\mathrm{LP}_{\mathrm{A}}-\mathrm{LP}_{\mathrm{B}}$ torque; Plot d: LP_{B}-GEN torque; Plot e: GEN-EXC torque.

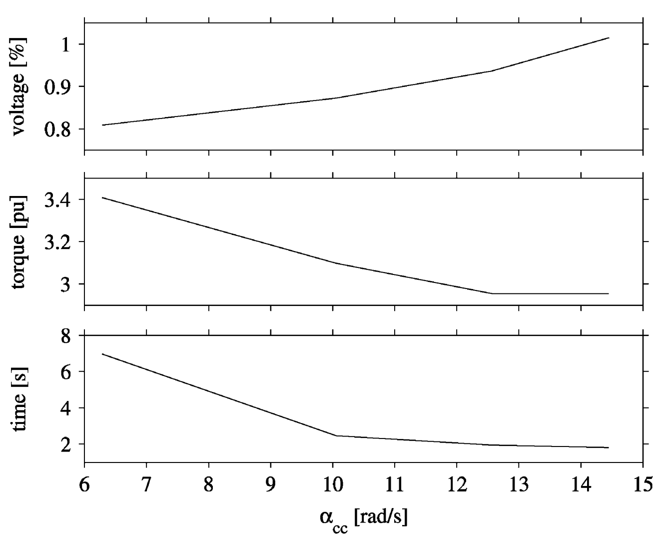

Fig. 16. Trend of injected voltage (top plot), peak $\mathrm{LP}_{\mathrm{B}}-\mathrm{GEN}$ torque (middle plot) and damping time (bottom plot) as function of bandwidth α_{cc}.

achieved with very low voltage injection, leading to a cost-effective solution to the problem of SSR.

REFERENCES

[1] "Terms, definitions and symbols for subsynchonous oscillations," *IEEE Trans. Power Apparat. Syst.*, vol. PAS-104, no. 6, pp. 1326–1334, Jun. 1985.

[2] P. Anderson, B. Agrawal, and J. V. Ness, *Subsynchronous Resonance in Power Systems*. New York: IEEE Press, 1989.

[3] K. Padiyar, *Analysis of Subsynchronous Resonance in Power systems*. Norwell, MA: Kluwer Academic Publishers, 1999.

[4] K. Padiyar and N. Prabhu, "Design and performance evaluation of subsynchronous damping controller with STATCOM," *IEEE Trans. Power Del.*, vol. 21, no. 3, pp. 1398–1405, Jul. 2006.

[5] L. S. Kumar and A. Ghosh, "Modeling and control design of a static synchronous series compensator," *IEEE Trans. Power Del.*, vol. 14, no. 4, pp. 1448–1453, Oct. 1999.

[6] B. T. Ooi and S. Z. Dai, "Series-type solid-state static VAR compensator," *IEEE Trans. Power Electron.*, vol. 8, no. 2, pp. 164–169, Apr. 1993.

[7] B. K. Perkins and M. R. Iravani, "Dynamic modeling of a TCSC with application to SSR analysis," *IEEE Trans. Power Syst.*, vol. 12, no. 4, pp. 1619–1625, Nov. 1997.

[8] K. Padiyar and R. Varma, "Damping torque analysis of static var system controllers," *IEEE Trans. Power Syst.*, vol. 6, no. 2, pp. 458–465, May 1991.

[9] "First benchmark model for computer simulation of subsynchronous resonance," *IEEE Trans. Power Appl. Syst.*, vol. PAS-96, no. 5, pt. 1, pp. 1565–1571, Sep. 1977.

[10] F. R. A. Jowder and B.-T. Ooi, "Series compensation of radial power systems by a combination of SSSC and dielectric capacitors," *IEEE Trans. Power Del.*, vol. 20, no. 1, pp. 458–465, Jan. 2005.
[11] G. Pillai, A. Ghosh, and A. Joshi, "Robust control of SSSC to improve torsional damping," in *Proc. 38th IEEE Power Eng. Soc. Winter Meeting*, Jan. 2001, vol. 3, pp. 1115–1120.
[12] K. R. Padiyar and N. Prabhu, "Analysis of subsynchronous resonance with three level twelve-pulse VSC based SSSC," in *Proc. Conf. Convergent Technol. Asia-Pacific Region (TENCON'03)*, Oct. 2003, vol. 1, pp. 76–80.
[13] M. Bongiorno, J. Svensson, and L. Ängquist, "Online estimation of subsynchronous voltage components in power systems," *IEEE Trans. Power Del.*, vol. 23, no. 1, pp. 410–418, Jan. 2008.
[14] L. Ängquist, "Synchronous Voltage Reversal Control of Thyristor Controlled Series Capacitor," Ph.D. dissertation, Dept. Elect. Eng., Royal Inst. Technol., Stockholm, Sweden, Sep. 2002.
[15] L. Harnefors and H.-P. Nee, "Model-based current control of ac-drives using the internal model control method," *IEEE Trans. Ind. Appl.*, vol. 34, no. 1, pp. 133–141, Jan. 1998.
[16] M. Bongiorno, L. Ängquist, and J. Svensson, "A novel control strategy for subsynchronous resonance mitigation using SSSC," *IEEE Trans. Power Del.*, to be published.
[17] P. Anderson and R. Farmer, *Series Compensation of Power Systems*. Encinitas, CA: PBLSH!, 1991.

Massimo Bongiorno (S'02) received the M.Sc. degree in electrical engineering from the University of Palermo, Palermo, Italy, in 2002 and the Lic.Eng. and Ph.D. degrees from Chalmers University of Technology, Göteborg, Sweden, in 2004 and 2007, respectively.

Since October 2007, he has been an Assistant Professor at Chalmers University of Technology. His interests include application of power electronics in power systems and power quality.

Jan Svensson (S'96–M'98) received the M.Sc., Lic. Eng., Ph.D., and D.Sc. degrees from Chalmers University of Technology, Göteborg, Sweden, in 1991, 1995, 1998, and 2002, respectively.

From 1998 to 2002, he was an Assistant Professor with the Department of Electric Power Engineering, Chalmers University of Technology. Currently, he is with ABB Power Technologies, Västerås, Sweden, involved in development of FACTS and HVDC transmission, especially design and control of light-concept devices. His interests include control of power electronics in power systems, power quality, energy storage, and wind power.

Lennart Ängquist (M'02) was born in Växjö, Sweden, in 1946. He received the M.Sc. degree from the Lund Institute of Technology, Lund, Sweden, in 1968 and the Ph.D. degree from the Royal Institute of Technology, Stockholm, Sweden, in 2002.

He has been employed by ABB (formerly ASEA), VästeråsSweden, in various technical departments. He was working with industrial and traction motor drives from 1974 to 1987. Thereafter, he has been working at FACTS applications in electrical power systems. He is an Adjunct Professor at the Royal Institute of Technology, Stockholm.